

A Density Functional Study of Bare and Hydrogenated Platinum Clusters

Ali Sebetci*

*Department of Computer Engineering,
Çankaya University, 06530 Balgat Ankara, Turkey*

(Dated: November 26, 2024)

Abstract

We perform density functional theory calculations using Gaussian atomic-orbital methods within the generalized gradient approximation for the exchange and correlation to study the interactions in the bare and hydrogenated platinum clusters. The minimum-energy structures, binding energies, relative stabilities, vibrational frequencies and the highest occupied and lowest unoccupied molecular-orbital gaps of Pt_nH_m ($n=1-5$, $m=0-2$) clusters are calculated and compared with previously studied pure platinum and hydrogenated platinum clusters. We investigate any magic behavior in hydrogenated platinum clusters and find that Pt_4H_2 is more stable than its neighboring sizes. Our results do not agree with a previous conclusion that 3D geometries of Pt tetramer and pentamer are unfavored. On the contrary, the lowest energy structure of Pt_4 is found to be a distorted tetrahedron and that of Pt_5 is found to be a bridge site capped tetrahedron which is a new global minimum for Pt_5 cluster. The successive addition of H atoms to Pt_n clusters leads to an oscillatory change in the magnetic moment of Pt_3 - Pt_5 clusters.

PACS numbers: 36.40.Cg, 71.15.Nc, 82.33.Hk

Keywords:

*Electronic address: asebetci@cankaya.edu.tr

I. INTRODUCTION

The study of hydrogen interaction with metals has gained an increased interest in the last decade [1, 2, 3, 4, 5, 6, 7]. The use of metal and semiconductor clusters as components of nanodevices, the development of cluster-based materials and the catalytic properties of clusters are the main reasons for the studies of interaction of atoms and molecules with clusters. Understanding hydrogen interaction with clusters is important because of two basic reasons: first, there is a great interest in developing novel hydrogen absorbing nanomaterials for fuel cell applications, second, many of the organic materials and biological systems contain hydrogen which are involved important catalytic reactions. In particular, platinum is one of the most important ingredients in the heterogeneous catalysis of hydrogenation as well as in the catalysis of the CO, NO_x, and hydrocarbons. Moreover, detailed investigations of the interaction between platinum clusters with hydrogen can contribute to the design of useful hydrogen storage devices. Therefore, it is of interest to understand the interaction of one and two H atoms on platinum clusters.

A brief summary of the previous theoretical and experimental studies on the pure platinum clusters can be found in our recent publications [8]. The following references can be added to them: Grönbeck and Andreoni [9] have presented a density functional theory (DFT) study of Au₂-Au₅ and Pt₂-Pt₅ clusters in the neutral and anionic states. Xiao and Wang [10] have studied Pt clusters of up to 55 atoms using DFT with a plane wave basis set and Tian et al. [11] have reported the geometrical and electronic structure of the Pt₇ cluster in a DFT study with a Gaussian type basis set. One of the earliest *ab initio* studies on the Pt-H₂ reaction was published by the group of Poulain [12] in 1986. The same group carried out theoretical studies on the Pt₂-H₂ [13], and Pt₄-H₂ [2] interactions later. Nakasuji et al. [14] accomplished an *ab initio* study on the reactions of the hydrogen molecule with small Pt_n ($n=1-3$) clusters. In 1987, Balasubramanian's [15] calculations on electronic states and potential energy surfaces of PtH₂ has been published. Later, he and Feng [16] have reported a study on the potential energy surfaces for the Pt₂-H and Pt-H interactions. The Pt₃-H₂ interactions have been studied by Dai et al. [17] and Cui et al. [18].

On the experimental side, molecular beam techniques have been used to investigate the hydrogen molecule interaction with metal surfaces [19]. The chemical reactivity of metal clusters in gas phase with hydrogen and deuterium has been studied with the laser vapor-

ization technique [20]. In a most recent study, Andrews et al. [21] have investigated the reaction of Pt atoms with H_2 in a laser-ablation experiment and have also performed some DFT calculations. In the experiments it is observed that the reactivity of the small metal clusters with the hydrogen and deuterium molecules strongly depends on the size of the small metal clusters [22]. Luntz et al. [23] found that there are reaction paths with or without very low barriers, leading to the H_2 dissociation on the Pt (111) surfaces.

In the present work, we report the results of first-principles total-energy calculations on small platinum clusters with up to two H atoms. We perform DFT calculations using Gaussian atomic-orbital methods within the generalized gradient approximation for the exchange and correlation to study the interactions in the bare and hydrogenated platinum clusters. The possible minima and ground states, binding energies (BE), relative stabilities, and the highest occupied and the lowest unoccupied molecular-orbital (HOMO-LUMO) gaps of the Pt_nH_m ($n=1-5$, $m=0-2$) clusters have been calculated. Vibrational frequency calculations for each optimized structure has been carried out to differentiate local minima from transition states. The results are compared with previously studied pure platinum and hydrogenated platinum clusters. Systematic growth in the atom number allows one to monitor the changes in the structure, dynamics, and electronic properties involved with the size of the clusters. This can provide an understanding of the nature of interaction between hydrogen and Pt clusters.

II. COMPUTATIONAL METHOD

DFT calculations have been performed by using version 4.7 of the NWChem program [24]. We have employed the LANL2DZ [25] basis set for the Pt atoms, which uses relativistic effective core potentials (ECP) to reduce the number of electrons explicitly considered in the calculation, and 6-311++G** basis set for the H atoms. The ECP parameters for platinum and the basis set, as well as similar basis sets to the one employed in this study for the hydrogen have been successfully used in many previous studies [7, 11, 12, 13, 21]. To examine the effect of the choice of the exchange-correlation functional, we have calculated the properties of H and Pt dimers and those of PtH diatomic molecule by using different functionals: We have employed PW91PW91 [26] and BPW91 [26, 27] functionals within the generalized gradient approximation (GGA), SVWN5 [28] functional within the local

density approximation (LDA), and B3LYP [26, 29] and B98PW91 [26, 30] methods as hybrid functionals. At the end of the examination which is discussed in the next section, we have chosen the BPW91 method to study Pt_nH_m clusters. The default NWChem geometry optimization convergence criteria were used in all cases. Initial structures have been relaxed without imposing any symmetry constraints. The final structures therefore include possible Jahn-Teller distortions. Whenever the optimized structure has had a symmetry other than C_1 , the relaxation process has been repeated with that symmetry constraints starting from the optimized geometry in order to get the electronic state. Spin-polarized calculations have been done for the first two multiplicities of the clusters up to Pt_4H . Thus, singlet and triplet states have been worked out for those having even number of electrons and doublet and quartet states have been worked out for those having odd number of electrons. In addition, we have also studied the quintet states of Pt_4H_2 , Pt_5 and Pt_5H_2 clusters, and sextet states of Pt_5H clusters. The reason for this is discussed in Sec. III D. All figures were produced by the ChemCraft graphics program [31].

A. Effect of Exchange-Correlation Functional

Table I displays the calculated and experimental values of the bond lengths, vibrational frequencies and BEs for H and Pt dimers and for PtH diatomic molecule. The experimental results of H_2 , Pt_2 , and PtH are from Refs. [32, 33], Refs. [34, 35, 36], and Refs. [32, 37], respectively. In our calculations, the hybrid method B3LYP has produced the nearest bond lengths to the experimental values of both H_2 and PtH molecules. However, it has resulted in the worst bond length (2.47 Å) for Pt_2 (experimental value is 2.33 Å). Therefore, it highly underestimates the BE of Pt dimer by calculating only a half of the experimental value. When a second hybrid functional B98PW91 is considered, it can be seen in Table I that although the results for Pt_2 are improved as compared to the results of the B3LYP method, it still overestimates the bond length and underestimates the BE of the dimer significantly. On the other hand, the SVWN5 LDA method has produced very good results for the bond lengths of all of the three molecules. However, when the BEs are taken into account, it is not favorable, too. It highly overestimates Pt_2 and PtH BEs. We have tried two GGA methods for the properties of the three diatomic molecules: PW91PW91 and BPW91. Both of them have resulted in nearly the same bond lengths which are excellent for H_2 and PtH,

and very good for Pt_2 . The errors in the bond length of Pt_2 produced by GGA methods are only 1.7%. They have also calculated reasonably good BEs for Pt_2 and PtH . PW91PW91 functional has produced a slightly better result for the BE of PtH than BPW91. However, the later has calculated much better Pt_2 BE than the former. Therefore, we have decided to employ BPW91 functional in the rest of our calculations. The error produced by the chosen method in the BE of H molecule (9.5%) is not very important in the present study since the H atoms in the Pt_nH_m clusters do not bind together as we discuss in the following sections. As a result, we have performed all the remaining computations of the hydrogenated Pt clusters at the BPW91/LANL2DZ and BPW91/6-311++G** levels of theory.

III. RESULTS AND DISCUSSION

A. Bare Pt Clusters: Pt_2 - Pt_5

We start to report the obtained results with bare Pt clusters.

Pt_2 : It can be seen from Table I and Table II that the chosen DFT method produces reasonably good results for the BE, vibrational frequency and the bond length of the Pt dimer. We have determined the electronic state of the dimer as $^3\Delta_g$ which is not consistent with Balasubramanian's [15] result that a $^3\Sigma_g^-$ is the ground state. The singlet state turns out to be 1.39 eV less stable than the triplet. Both of the references [9] and [10] have reported the ground state of the dimer as a triplet, however none of them has given any electronic state. Xiao and Wang [10] have calculated 3.52 eV BE, 2.34 Å bond distance and 0.81 eV HOMO-LUMO gap in their DFT study with ultrasoft pseudopotentials. The best energy and bond length values of Grönbeck and Andreoni [9] obtained by employing BLYP exchange correlation functional are 3.58 eV and 2.32 Å, respectively. For both of these studies, the bond distance values are closer to the experimental data (2.33 Å) than our result (2.37 Å), however the method employed in this work results better in the energy since it calculates 3.36 eV BE which is closer to the experimental data (3.14 eV) than the previous calculations. Balasubramanian [15] has reported the obtained Pt-Pt distance as 2.46 Å which is the worst among all of the above mentioned references. We have calculated 1.32 eV HOMO-LUMO gap which is significantly higher than the one given in Ref. [10]. Our result for the β spin HOMO-LUMO gap (0.33 eV) is in agreement with the calculation

of Tian et al. [11] (0.3 eV).

Pt₃: The isomeric structures, symmetries, ground electronic states, total BEs, HOMO-LUMO gaps (α spin), and the highest and the lowest vibrational frequencies of Pt₂-Pt₅ clusters are given in Table II. The pictures of these isomers and the bond lengths (in Å) in these structures are presented in Fig. 1. We have studied the equilateral and isosceles triangle structures of the Pt trimer, and found out that the optimized bond lengths of these two geometries are very similar (see Fig. 1 (3-1) and (3-2)). Therefore, the energy separation between them is very small. All Pt-Pt distances in the equilateral triangle are 2.53 Å which can be compared with the result of Grönbeck and Andreoni [9] (2.41 Å). The ground electronic state of the D_{3h} symmetry is $^3E''$ whereas that of C_{2v} symmetry is 3B_2 . The BEs and the HOMO-LUMO gaps for both of these structures are 6.57 eV and 1.05 eV, respectively.

Pt₄: We have identified three stable structures of Pt₄: a distorted tetrahedron (4-1), an out of plane rhombus (4-2), and a planar Y-like shape (4-3). A square isomer has been found to be a first order transition state in our calculations. The distorted tetrahedron with C_2 symmetry and 3B electronic state is 0.1 eV more stable than the rhombus, whereas the BE of the rhombus is 0.29 eV higher than the BE of the third isomer. The HOMO-LUMO gaps and the lowest and highest vibrational frequencies of these clusters can be found in Table II. Previously, Grönbeck and Andreoni [9] have reported the global minimum to be a slightly out of plane rhombus in the triplet. Xiao and Wang [10] have found a distorted tetrahedron with C_s symmetry as the lowest energy structure in their plane wave calculations. Dai and Balasubramanian [38] have performed MRSDCI calculations and a regular tetrahedron in a triplet state was determined to be the ground state.

Pt₅: A bridge site capped tetrahedron (5-1), a rhombus pyramid (5-2), a trigonal bipyramid (5-3), an X-like (5-4) and an W-like (5-5) geometries are the low-energy structures of Pt₅. This is the first time, to the best of our knowledge, that the bridge site capped tetrahedron (5-1) is identified as the global minimum of Pt₅. It is in the quintet state and 0.09 eV more stable than the second isomer. The second isomer (rhombus pyramid) is also in the quintet state, whereas the other three locally stable structures are in triplet. The HOMO-LUMO gap (0.69 eV) of the lowest energy structure (5-1) is also higher than that of the other isomers. Therefore, it is expected to be more stable than the other structures. The BE of the rhombus pyramid is 0.07 eV higher than the BE of the trigonal bipyramid.

The energy separation of the almost planar X-like and W-like structures from the 3D configurations is more than 0.04 eV. In Ref. [9], BLYP calculations have predicted the lowest energy isomer to be the planar W-like shape and LDA calculations have placed a distorted square pyramid at low energies. In Ref. [10], the trigonal bipyramid has been found as the global minimum in the quintet state.

According to the results presented here, the claim that 3D geometries for Pt tetramer and pentamer are unfavored is not true. In addition, the HOMO-LUMO gaps for Pt₂-Pt₅ obtained in our calculations (1.32, 1.05, 0.44, and 0.69 eV, respectively) are generally much greater than the previous calculations (0.7, 0.2, 0.3, and 0.2 eV in Ref. [9], and 0.81, 0.034, 0.28, and 0.63 eV in Ref. [10]).

B. One and Two Hydrogens on Pt Clusters

The relaxed structures and bond lengths of one and two H atoms on small Pt clusters are shown in Fig. 2, while the symmetries, electronic states, BEs, HOMO-LUMO gaps (α spin) and the highest and the lowest vibrational frequencies are given in Table III.

PtH: Considering first the interaction of H with a Pt atom will be instructive. We have calculated the BE of the PtH molecule in the doublet state as 3.28 eV, which is close to the experimental data [32] of 3.44 eV. In fact, as discussed by Balasubramanian and Feng [16] the experimental value should be regarded as only an upper bound. They have reported the ground state BE as 3.11 eV by employing the CASSCF/SOCI/RCI method in 1989 [16]. We have identified the electronic ground state of the molecule as $^2\Delta$ which is in agreement with both the experimental [37] and Balasubramanian's theoretical results [16]. Andrews et al. [21] have investigated PtH_n ($n=1-3$) clusters by employing the B3LYP and BPW91 density functionals with 6-311+G**, 6-311++G(3df,3pd) and aug-cc-pVTZ basis sets for H, and LANL2DZ and SDD pseudopotentials for Pt. In their study, the ground state has been determined as $^2\Sigma^+$, however no BE has been given. We have computed the bond length of PtH as 1.528 Å which is also in very good agreement with the experimental value [37] of 1.529 Å. It is determined as 1.55 Å in Ref. [16] and as 1.531 Å in Ref. [21]. When the vibrational frequency is considered, the experimental data [37] is 2294 cm⁻¹. Our result is 2420 cm⁻¹ whereas Ref. [16] and Ref. [21] have reported 2177 and 2370 cm⁻¹, respectively. It should be noted here that all frequencies given in this work are determined without using

any scale factor. If they were scaled by a proper factor for the chosen method, they would be more accurate. The HOMO-LUMO gap of PtH is 3.02 eV which is the largest gap among all the clusters we have studied here. Since the total energy of Pt₂ and H₂ (7.66 eV) is bigger than the energy of 2PtH (6.56 eV), one can expect the abundance of the PtH molecule in an environment of atomic hydrogen rather than in an environment of molecular hydrogen.

PtH₂: PtH₂ has a waterlike structure as shown in Fig. 2 (1b) with an angle of 85.9°. This angle was reported previously as 85° by Balasubramanian [15] and as 85.7° by Andrews et al. [21]. As in the case of the angle, our result for the bond length (1.517 Å) is in very good agreement with the previous calculation (1.520 Å) [21]. All of these studies (Ref. [15], Ref. [21], and the present paper) identify the ground state of the PtH₂ molecule to be ¹A₁. It can be seen from Table III that the BE of H on PtH (3.58 eV) is 0.30 eV higher than the BE of H on Pt atom (3.28 eV). Thus, PtH₂ is a bit more stable than PtH when H separations from these molecules are considered. Although the HOMO-LUMO gap of PtH₂ (2.49 eV) is smaller than that of PtH, it is still a big gap. We have found PtH₂ to be 6.86 eV more stable than the ground state Pt atom and two ground state H atoms. In order to dissociate H₂ molecule from PtH₂, 2.55 eV is needed. This energy may be compared with earlier calculations: 2.15 eV [21], 1.73 eV [14], and 2.04 - 2.21 eV [15]. We have determined the lowest, middle and the highest vibrational frequencies as 793, 2455, 2490 cm⁻¹. In Ref. [21], the corresponding frequencies are computed in the following ranges by employing different methods and basis sets: 784 - 805, 2414 - 2456, 2455 - 2513 cm⁻¹. The H-H distance in PtH₂ is 2.07 Å, which is significantly greater than the bond length of H₂ (0.74 Å). Therefore, the interaction between Pt and H₂ is dissociative.

Pt₂H: There are two possible ways of H bonding on the Pt dimer: on the bridge site (Fig. 2 (2b) which is an isosceles triangle) and on the top site (Fig. 2 (2c) which is a planar V-like shape with C_s symmetry). Different electronic states of the bridge structure have been studied in Ref. [16] before and a ²A₂ state has been identified as the ground state, which is in full agreement with our result. 2.53 Å of the Pt-Pt distance and 1.75 Å of the Pt-H distance given in that study can be compared with the present results of 2.50 Å and 1.71 Å, respectively. We have determined the ground state of the top structure to be a ⁴A'' state. The energy difference between the quartet and doublet states of this geometry is 0.50 eV. The BEs of H on the bridge and top sites of Pt₂ are 2.73 eV and 2.25 eV, respectively. Since these energies are particularly high it can be concluded that Pt₂ is a reactive molecule.

The bonding on the bridge site is 0.48 eV more favorable than the bonding on the top site. On the other hand, the HOMO-LUMO gap of (2c) structure (2.57 eV) is much greater than that of (2b) structure (1.26 eV). Thus, the further reaction of the isosceles triangle to make Pt_2H_2 can occur easier than that of the V-like structure. In the V-like structure, the Pt-Pt and Pt-H distances are reduced to 2.44 Å and 1.56 Å.

Pt_2H_2 : We have identified three stable structures of Pt_2H_2 ; (i) both H atoms are on the bridge site (Fig. 2 (2d)), (ii) both of them are on the top sites of different Pt atoms (Fig. 2 (2e)), and (iii) both of them are on the top site of the same Pt atom (Fig. 2 (2f)). An initial geometry of a bridge-top configuration takes the (2e) form at the end of the optimization process. The singlet states of all of these three structures are more stable than their triplet states. Among the three local minima, (2e) form has the biggest BE (9.29 eV). The HOMO-LUMO gap of the (2f) form (0.09 eV) is significantly small, therefore it is expected to react further to make Pt_3H_2 or Pt_2H_3 . The H-H distance in (2f) is 2.05 Å which is again much bigger than the bond distance in the H molecule. Therefore, the H adsorption on Pt dimer is also dissociative.

Pt_3H : Interaction of H on Pt_3 is slightly favorable on the bridge site (Fig. 2 (3b)) as compared to the top site (Fig. 2 (3c)) by 0.06 eV. The HOMO-LUMO gap in the (3b) form (0.66 eV) is also greater than the gap in the (3c) form (0.19 eV). The ground states of both of these structures are doublet. The H BEs in these geometries are 2.63 eV and 2.57 eV respectively, which are relatively small when compared to the most of the BEs in the other Pt_nH_m clusters. The Pt-H distance in the bridge site (1.71 Å, (3b)) is very similar to the corresponding bridge site distances of the previous clusters, that is Pt-H distances in Pt_2H (2b) and Pt_2H_2 (2d). The same is true for the typical 1.53 Å Pt-H top site distance in the (3c) form which is very close to the Pt-H distances in the (1a), (1b), (2e), and (2f) structures. The only exception of this is the 1.56 Å Pt-H bond length in the (2c) form which can be related to the fact that (2c) structure is a quartet although all the other Pt_nH clusters listed above are doublets. In our calculations, we have not found any local minima of Pt_3H in which H has a coordination number of three or more.

Pt_3H_2 : We have identified 9 different local minima of Pt_3H_2 ; three bridge-bridge configurations (Fig. 2 (3d)-(3f)), four bridge-top configurations (Fig. 2 (3g)-(3j)), and two top-top configurations (Fig. 2 (3k), (3l)). In the (3d) geometry the two H atoms are on the same bridge site, whereas in the (3e) and (3f) forms they are on the neighboring sites. The dif-

ference between (3e) and (3f) is that in the former case H atoms are on the opposite sides of the Pt_3 plane, whereas in the later case they are not. Among the four bridge-top configurations, (3h) is the only one having a Pt atom bonding to both of the H atoms. In the (3g) and (3j) geometries the bridge and top site H atoms are on the opposite and on the same sides of the Pt_3 plane, respectively. In the (3i) case, all the atoms of the cluster are on the same plane. In one of the top-top configuration, the H atoms are bonded to different Pt atoms (3k). They are bonded to the same Pt atom in the other one (3l). The top-top configurations have greater BEs than all the other isomers (see Table III). When the two H atoms are bonded to the top site of the same Pt atom (3l), the ground state is a triplet which is different from the singlet (2f) structure of Pt_2H_2 . The (3l) structure has the greatest BE and HOMO-LUMO gap, and therefore it is the most stable Pt_3H_2 cluster that we have investigated in the present work. The H-H distance in it is 1.75 Å. The BE for 2H is 5.51 eV and it is significantly higher than the dissociation energy of H_2 (4.75 eV). Accordingly, hydrogen is likely to be dissociated on Pt_3 as well as on Pt_2 . Among the bridge-top configurations, (3h) structure has higher BE than the others. The bridge-top isomers of the Pt_3H_2 cluster are generally more stable than its bridge-bridge isomers except that (3f) geometry has greater BE than (3i).

Pt_4H & Pt_4H_2 : H prefers to bind to the ground state Pt tetramer on the top site. The isomer with H on the top site (Fig. 2 (4c)) is a quartet and its BE is 0.3 eV greater than that of the isomer with H on the bridge site (Fig. 2 (4b)) which is a doublet. The HOMO-LUMO gap of (4c) is also greater than that of (4b) (see Table III). Thus, (4c) structure is expected to be more stable. In the case of 2H, the most stable structure is a top-top configuration (Fig. 2 (4h)) which is similar to the Pt_3H_2 case. The HOMO-LUMO gap of this structure is 0.94 eV and it is higher than that of all the other Pt_4H_2 isomers. The H-H distance in (4h) is 1.95 Å. The 2H BE is 5.80 eV. Thus, the H absorption is again dissociative. The BEs of the neighbor bridge-bridge configuration (4d) and the opposite bridge-bridge configuration (4e) are nearly the same. However, (4d) is a triplet whereas (4e) is a singlet. For the bridge-top configurations, the neighboring structure (4f) is 0.1 eV more stable than the opposite structure (4g).

Pt_5H & Pt_5H_2 : H can bind to the ground state Pt pentamer on three different bridge and two different top sites. Top site bonding is favorable in BE: (5f) is the lowest energy structure. However the HOMO-LUMO gaps of the bridge site bonded structures are higher

than those of top site bonded structures. All Pt_5H isomers in Table III are in the quartet states. For the bonding of 2H, we have identified three bridge-bridge, four bridge-top, and three top-top locally stable configurations. In each of these 10 optimization processes, we have started from different H locations on the lowest energy structure (5-1) of the Pt_5 cluster. However, in three of them (5-1) configuration of the 5 Pt atoms changed into some other topologies at the end of the relaxation: The (5i) and (5p) geometries are based on trigonal bipyramid and the (5o) resembles to rhombus pyramid. In agreement with the general trend, the most stable Pt_5H_2 isomer is the (5p) top-top structure with the highest BE and the highest HOMO-LUMO gap. The H-H distance in (5p) is 1.91 Å and the 2H BE is 5.59 eV. Thus, the H absorption is still dissociative. While the ground state Pt_5H_2 cluster (5p) and three other isomers ((5i), (5k), and (5m)) are in quintet states, the other six isomers are in triplet states. Similar to the previous clusters, generally bridge-top configurations have higher BEs than bridge-bridge structures.

C. Fragmentation Behavior

Figure 3 shows the plot of the BE of one and two H atoms on the lowest energy isomers of the Pt clusters. The H BE is large for most clusters and in particular for clusters with 1 and 4 Pt atoms. This is similar when 2H BEs are considered. The clusters with 1, and 4 Pt atoms have larger BEs for 2H compared to their neighboring sizes. We have further studied the stability of these clusters from the fragmentation channels in which a Pt atom, or a Pt_2 , or PtH molecule is one of the fragments. The fragmentation energies of all of these channels are listed in Table IV. It is noted that the fragmentation energies are the largest for Pt_4H_2 in Pt and PtH fragmentation channels. Therefore, we expect it to be the most stable species. For the Pt_2 fragmentation, Pt_5H_2 has the highest fragmentation energy. On the other hand, Pt_2H_2 and Pt_3H_2 have the lowest fragmentation energies for this channel.

D. Magnetic Moment of Pt_nH_m Clusters

In this section we discuss the change in the magnetic moment of the hydrogenated platinum clusters when successive H atoms are added to the bare Pt clusters. The magnetic moments and the majority and minority spin LUMO energies of the lowest energy structures

for Pt_nH_m ($n = 1-5$, $m = 0-2$) clusters are presented in Table V. It can be seen in Table V that the successive H addition to Pt atom and Pt dimer reduces the magnetic moment as in the case of H absorption in bulk Pt. However, when the successive H additions to the Pt trimer and pentamer are considered, it is observed that as the magnetic moments decrease in the first additions, they increase in the second ones. For the tetramer, the magnetic moment increases in the first addition and decreases in the second. Thus, the magnetic moments of certain small Pt clusters exhibit an oscillatory change in the successive addition of H atoms.

The results obtained in this study confirm the explanation of Ashman et al. [4] that this situation can be understood by looking at the LUMO energy differences between the majority and minority spin electrons ($\delta E = \text{minority spin LUMO energy} - \text{majority spin LUMO energy}$). When the minority spin LUMO energy is much less than the majority spin LUMO energy (when δE is highly negative), the additional electron goes to the spin state with lowest LUMO, and reduces the magnetic moment to decrease the cluster's total energy. This is what happens when successive H atoms are added to Pt atom and dimer. However, if LUMO of minority is slightly less than LUMO of majority (if δE is greater than a certain value which is around -0.227 eV for Pt-H clusters), the additional electron may go to majority manifold since the exchange coupling could lead to a rearrangement of the manifolds. This explains the increases in the magnetic moments when H atoms are added to the Pt_3H and Pt_4 clusters. It should be noted here that nearly a half of the Pt_3H_2 isomers in Table III are in the singlet, and the others are in the triplet states. Similarly, one of the Pt_4H isomer is in the doublet and the other is in the quartet states. For Pt_5H , the δE is even positive and therefore we expect that H addition will most probably increase the magnetic moment. In fact, this expectation is confirmed in our results since the lowest energy isomer of the Pt_5H_2 is found to be in the quintet state.

IV. SUMMARY

In summary, we have presented results of studies on the interactions in the bare and hydrogenated platinum clusters. We find that H interacts strongly with Pt clusters. The interaction of H_2 molecule with any of the Pt clusters studied in the present work is likely to be dissociative. H atoms can bond to Pt clusters either on a bridge site or on a top site. We do not find any 3-fold bonding of H to Pt clusters. In general, a top site bonding is more

favorable than a bridge site bonding. Therefore, for the bonding of two H atoms, top-top configurations are more stable than bridge-top and bridge-bridge configurations. Among all the clusters we have investigated, we find that Pt_4H_2 is the best candidate to be the most stable one. We do not agree with a previous claim that 3D geometries of Pt tetramer and pentamer are unfavored. We have identified a distorted tetrahedron and a bridge site capped tetrahedron as the lowest energy structures of Pt_4 and Pt_5 , respectively. We have also shown that the successive addition of H atoms to Pt clusters decreases the magnetic moments of the Pt atom and Pt dimer, whereas it leads to an oscillatory change in the magnetic moment of Pt_3 - Pt_5 clusters.

Acknowledgments

This work is financially supported by The Scientific and Technological Research Council of Turkey, Grant no. TBAG-HD/38 (105T051). I would also like to thank to Dr. Ersen Mete for discussion and comments as well as his valuable computational supports.

-
- [1] Y. Okamoto, Chem. Phys. Lett. 405, 79 (2005).
- [2] E. Poulain, J. Benitez, S. Castillo, V. Bertin, A. Cruz, J. Mol. Struc. THEOCHEM 709, 67 (2004).
- [3] W.M. Bartczak, J. Stawowska, Struc. Chem. 15, 447 (2004).
- [4] C. Ashman, S.N. Khanna, M.R. Pederson, Chem. Phys. Lett. 368, 257 (2003).
- [5] J. Moc, D.G. Musaev, K.J. Morokuma, J. Phys. Chem. A 107, 4929 (2003).
- [6] D.S. Mainardi, P.B. Balbuena, J. Phys. Chem. A. 107, 10370 (2003).
- [7] H. Kawamura, V. Kumar, Q. Sun, Y. Kawazoe, Phys. Rev. B 65, 045406 (2001).
- [8] A. Sebetci and Z.B. Güvenç, Surf. Sci. 525, 66 (2003); Eur. Phys. J. D, 30, 71 (2004); Modelling Simul. Mater. Sci. Eng. 13, 683, (2005).
- [9] H. Grönbeck, W. Andreoni, Chem. Phys. 262, 1 (2000).
- [10] L. Xiao, L. Wang, J. Phys. Chem. A 108, 8605 (2004).
- [11] W.Q. Tian, M. Ge, B.R. Sahu, D. Wang, T. Yamada, S. Mashiko, J. Phys. Chem. A 108, 3806 (2004).
- [12] E. Poulain, J. Garcia-Prieto, M.E. Ruiz, O. Novaro, Int. J. Quantum. Chem. 29, 1181 (1986).
- [13] E. Poulain, V. Bertin, S. Castillo, A. Cruz, J. Mol. Catal. A: Chem. 116, 385 (1997).
- [14] H. Nakasuji, Y. Matsuzaki, T. Yonezawa, J. Chem. Phys. 88, 5759 (1988).
- [15] K. Balasubramanian, J. Chem. Phys. 87, 2800 (1987); J. Chem. Pyhs. 87, 6573 (1987); J. Chem. Pyhs. 94, 1253 (1991).
- [16] K. Balasubramanian, P. Y. Feng, J. Chem. Phys. 92, 541 (1990).
- [17] D. Dai, W. Liao, K. Balasubramanian, J. Chem. Phys. 102, 7530 (1995).
- [18] Q. Cui, D.G. Musaev, K. Morokuma, J. Phys. Chem. A 108, 8418 (1998).
- [19] P. Samson, A. Nesbitt, B.E. Koel, A. Hodgson, J. Chem. Phys 109, 3255 (1998).
- [20] A. Kaldor, D.M. Cox, M. R. Zakin, Adv. Chem. Phys. 70, 211 (1988).
- [21] L. Andrews, X. Wang, L. Manceron, J. Chem. Phys. 114, 1559 (2001).
- [22] M.B. Knickelbein, G.M. Koretsky, K.A. Jackson, M.R. Pederson, Z. Hajnal, J. Chem. Phys. 109, 10692 (1998).
- [23] A.C. Luntz, J.K. Brown, M.D. Williams, J. Chem. 93, 5240 (1990).
- [24] E. Apra, T. L. Windus, T. P. Straatsma et al. NWChem, A Computational Chemistry Package

- for Parallel Computers, Version 4.7 (2005).
- [25] P.J. Hay, W.R. Wadt, J. Chem. Phys. 82, 299 (1985).
 - [26] J.P. Perdew, J.A. Chevary, S.H. Vosko, K.A. Jackson, M.R. Pederson, D.J. Singh, C. Fiolhais, Phys. Rev. B 46, 6671 (1992).
 - [27] A.D. Becke, Phys. Rev. A 38, 3098 (1988).
 - [28] J.C. Slater, Quantum Theory of Molecules and Solids (McGraw-Hill, New York, 1974).
 - [29] A.D. Becke, J. Chem. Phys. 98, 5648 (1993).
 - [30] H.L. Schmider, A.D. Becke, J. Chem. Phys. 108, 9624 (1998).
 - [31] <http://www.chemcraftprog.com>.
 - [32] K.P. Huber, G. Herzberg, Molecular Spectra and Molecular Structure. IV. Constants of Diatomic Molecules (Van Nostrand Reinhold, New York, 1979).
 - [33] K.P. Huber, in American Institute of Physics Handbook, edited by D.E. Gray (McGraw-Hill, New York, 1972).
 - [34] M.B. Airola, M.D. Morse, J. Chem. Phys. 116, 1313 (2002).
 - [35] J.C. Fabbri, J.D. Langenberg, Q.D. Costello, M.D. Morse, L. Karlsson, J. Chem. Phys. 115, 7543 (2001).
 - [36] S. Taylor, G.W. Lemire, Y.M. Hamrick, Z. Fu, M.D. Morse, J. Chem. Phys. 89, 5517 (1988).
 - [37] M.C. McCarthy, R.W. Field, R. Engleman, P.F. Bernath, J. Mol. Spectrosc. 158, 208 (1993).
 - [38] D. Dai, K. Balasubramanian, J. Chem. Phys. 103, 648 (1995).

TABLE I: Comparison of the calculated and experiment properties of H_2 , Pt_2 , and PtH . Experimental values for the bond lengths, vibrational frequencies and binding energies of H_2 , Pt_2 , and PtH are from Refs. [32, 33], Refs. [34, 35, 36], and Refs. [32, 37], respectively.

	Bond length (\AA)			Vibrational frequency (cm^{-1})			Binding energy (eV)		
	H_2	Pt_2	PtH	H_2	Pt_2	PtH	H_2	Pt_2	PtH
Expt	0.74	2.33	1.53	4360	223	2294	4.75	3.14	3.44
PW91PW91	0.75	2.37	1.53	4333	235	2423	4.27	3.51	3.35
B3LYP	0.74	2.47	1.53	4419	205	2423	4.49	1.57	3.33
SVWN5	0.77	2.33	1.52	4189	252	2475	4.64	4.37	4.12
BPW91	0.75	2.37	1.53	4345	234	2420	4.30	3.36	3.28
B98PW91	0.74	2.45	1.52	4439	210	2443	4.35	2.15	3.61

TABLE II: Isomeric structure properties of Pt_n ($n=2-5$) clusters.

Cluster	Structure	Symmetry	Ground state	Total BE (eV)	HOMO-LUMO gap (eV)	ω_l and ω_h ^a (cm^{-1})
Pt_2	linear	$D_{\infty h}$	$^3\Delta_g$	3.36	1.32	234
(3-1) Pt_3	equilateral triangle	D_{3h}	$^3E''$	6.57	1.05	118, 221
(3-2)	isosceles triangle	C_{2v}	3B_2	6.57	1.05	118, 220
(4-1) Pt_4	distorted tetrahedron	C_2	3B	9.76	0.44	74, 215
(4-2)	out of plane rhombus	C_{2v}	3A_2	9.66	0.40	28, 207
(4-3)	Y-like	C_s	$^3A''$	9.37	0.48	25, 262
(5-1) Pt_5	bridge site capped tetrahedron	C_2	5B	13.20	0.69	29, 206
(5-2)	rhombus pyramid	C_{2v}	5A_2	13.11	0.30	32, 207
(5-3)	trigonal bipyramid	C_s	$^3A''$	13.04	0.41	44, 207
(5-4)	X-like	D_{2h}	$^3B_{2u}$	13.00	0.60	22, 254
(5-5)	W-like	C_1	3A	12.86	0.30	22, 227

^aLowest and highest vibrational frequencies

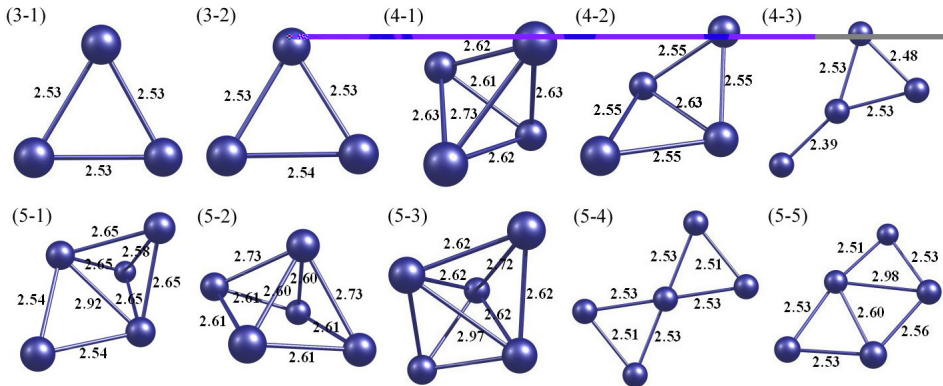


FIG. 1: Relaxed structures of Pt_n ($n=3-5$). All distances are in \AA .

TABLE III: Properties of Pt_nH_m ($n=1-5$ and $m=0-2$) clusters. Location of H is represented by symbols b and t which mean bridge and top site, respectively.

	Cluster	Location of H	Symmetry	Ground state	Total BE (eV)	BE of H (eV)	HOMO-LUMO gap (eV)	ω_l and ω_h^a (cm^{-1})
(1a)	PtH		$C_{\infty v}$	$^2\Delta$	3.28	3.28	3.02	2420
(1b)	PtH ₂		C_{2v}	1A_1	6.86	6.86	2.49	793, 2490
(2a)	Pt ₂		$D_{\infty h}$	$^3\Delta_g$	3.36		1.32	234
(2b)	Pt ₂ H	b	C_{2v}	2A_2	6.09	2.73	1.26	192, 1636
(2c)		t	C_s	$^4A''$	5.61	2.25	2.57	183, 2213
(2d)	Pt ₂ H ₂	b-b	C_{2v}	1A_1	8.95	5.59	0.94	180, 1646
(2e)		t-t (1)	C_2	1A	9.29	5.93	0.87	193, 2451
(2f)		t-t (2)	C_s	$^1A'$	8.49	5.13	0.09	202, 2397
(3a)	Pt ₃		D_{3h}	$^3E''$	6.57		1.05	118, 221
(3b)	Pt ₃ H	b	C_s	$^2A''$	9.20	2.63	0.66	115, 1715
(3c)		t	C_1	2A	9.14	2.57	0.19	138, 2449
(3d)	Pt ₃ H ₂	b-b (1)	C_{2v}	1A_1	11.70	5.13	0.59	120, 1505
(3e)		b-b (2)	C_2	3A	11.39	4.82	0.24	116, 1627
(3f)		b-b (3)	C_s	$^1A'$	11.80	5.23	0.50	62, 1499
(3g)		b-t (1)	C_s	$^3A''$	11.97	5.40	0.71	105, 2266
(3h)		b-t (2)	C_1	1A	11.98	5.41	0.37	105, 2246
(3i)		b-t (3)	C_s	$^1A'$	11.57	5.00	0.17	113, 2237
(3j)		b-t (4)	C_s	$^3A''$	11.92	5.35	0.65	101, 2291
(3k)		t-t (1)	C_2	1A	12.07	5.50	0.45	89, 2317
(3l)		t-t (2)	C_s	$^3A''$	12.08	5.51	1.03	107, 2316
(4a)	Pt ₄		C_2	3B	9.76		0.44	74, 215
(4b)	Pt ₄ H	b	C_1	2A	12.36	2.60	0.27	39, 1277
(4c)		t	C_1	4A	12.66	2.90	0.59	83, 2232
(4d)	Pt ₄ H ₂	b-b (1)	C_s	$^3A''$	15.05	5.29	0.38	68, 1334
(4e)		b-b (2)	C_s	$^1A'$	15.06	5.30	0.40	69, 1286
(4f)		b-t (1)	C_1	3A	15.38	5.62	0.63	70, 2174
(4g)		b-t (2)	C_1	3A	15.28	5.52	0.56	51, 2168
(4h)		t-t	C_s	$^3A'$	15.56	5.80	0.94	71, 2264
(5a)	Pt ₅		C_2	5B	13.20		0.69	29, 206
(5b)	Pt ₅ H	b (1)	C_2	4B	15.83	2.78	0.67	25, 1359
(5c)		b (2)	C_1	4A	15.75	2.70	0.58	28, 1267
(5d)		b (3)	C_1	4A	15.71	2.66	0.75	16, 1350
(5e)		t (1)	C_1	4A	15.85	2.80	0.45	24, 2234
(5f)		t (2)	C_1	4A	15.89	2.84	0.45	27, 2203
(5g)	Pt ₅ H ₂	b-b (1)	C_1	3A	18.32	5.27	0.49	27, 1397
(5h)		b-b (2)	C_1	3A	18.29	5.09	0.67	17, 1364
(5i)		b-b (3)	C_1	5A	18.44	5.24	0.47	43, 1344
(5j)		b-t (1)	C_1	3A	18.49	5.29	0.41	26, 2232
(5k)		b-t (2)	C_s	$^5A''$	18.54	5.34	0.66	27, 2279
(5l)		b-t (3)	C_1	3A	18.54	5.34	0.43	27, 2207
(5m)		b-t (4)	C_1	5A	18.31	5.26	0.52	19, 2263
(5n)		t-t (1)	C_1	3A	18.55	5.35	0.32	17, 2261
(5o)		t-t (2)	C_1	3A	18.64	5.44	0.29	29, 2288
(5p)		t-t (3)	C_s	$^5A''$	18.79	5.59	0.67	64, 2323

^aLowest and highest vibrational frequencies

TABLE IV: Fragmentation energies of Pt_nH_m clusters. Energies are given in eV and a positive value means that the parent cluster has a larger BE than the sum of the BEs of the products.

	Cluster (Pt_nH_m)	$\text{Pt}_{n-1}\text{H}_m + \text{Pt}$	$\text{Pt}_{n-2}\text{H}_m + \text{Pt}_2$	$\text{Pt}_{n-1}\text{H}_{m-1} + \text{PtH}$
(2b)	Pt_2H	2.81	2.73	2.81
(2e)	Pt_2H_2	2.43	1.63	2.73
(3b)	Pt_3H	3.12	2.57	2.57
(3l)	Pt_3H_2	2.79	1.86	2.71
(4c)	Pt_4H	3.45	3.21	2.81
(4h)	Pt_4H_2	3.48	2.91	3.07
(5f)	Pt_5H	3.23	3.32	2.85
(5p)	Pt_5H_2	3.23	3.35	2.85

TABLE V: The majority and minority LUMO levels

	Cluster	Magnetic moment	Majority LUMO (eV)	Minority LUMO (eV)	δE (eV)
	Pt	2	-1.155	-5.430	-4.275
(1a)	PtH	1	-2.660	-5.150	-2.490
(1b)	PtH_2	0	-2.821	-2.821	0.000
(2a)	Pt_2	2	-4.427	-5.108	-0.681
(2b)	Pt_2H	1	-4.127	-5.059	-0.932
(2e)	Pt_2H_2	0	-4.426	-4.426	0.000
(3a)	Pt_3	2	-4.083	-4.803	-0.720
(3b)	Pt_3H	1	-4.201	-4.428	-0.227
(3l)	Pt_3H_2	2	-4.385	-5.124	-0.739
(4a)	Pt_4	2	-4.104	-4.215	-0.111
(4c)	Pt_4H	3	-4.401	-4.552	-0.151
(4h)	Pt_4H_2	2	-4.345	-4.524	-0.179
(5a)	Pt_5	4	-4.428	-4.600	-0.172
(5f)	Pt_5H	3	-4.743	-4.682	0.061
(5p)	Pt_5H_2	4	-4.699	-5.087	-0.388

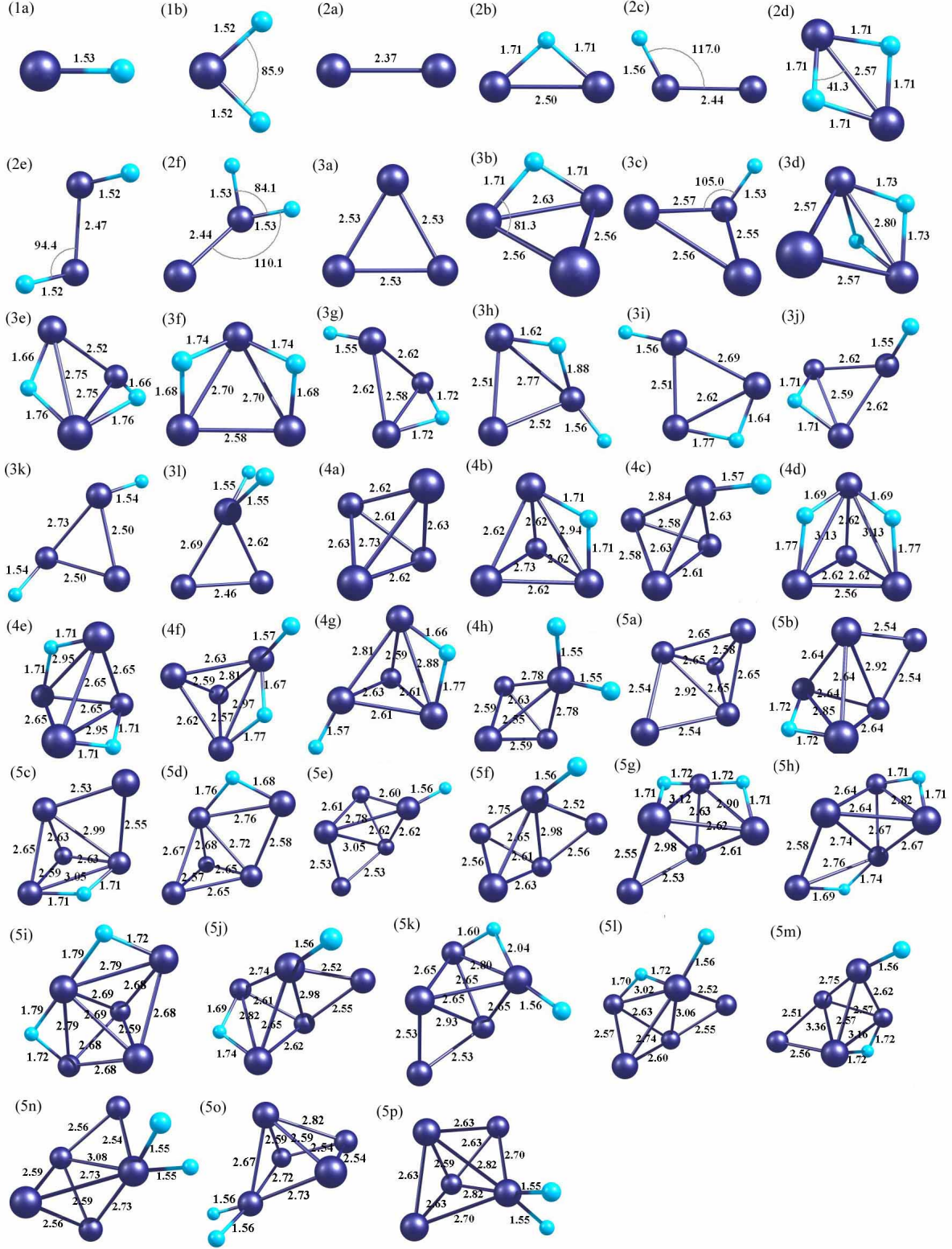


FIG. 2: Relaxed structures of Pt_nH_m ($n=1-5$ and $m=0-2$). Distances are in Å and angles are in degree.

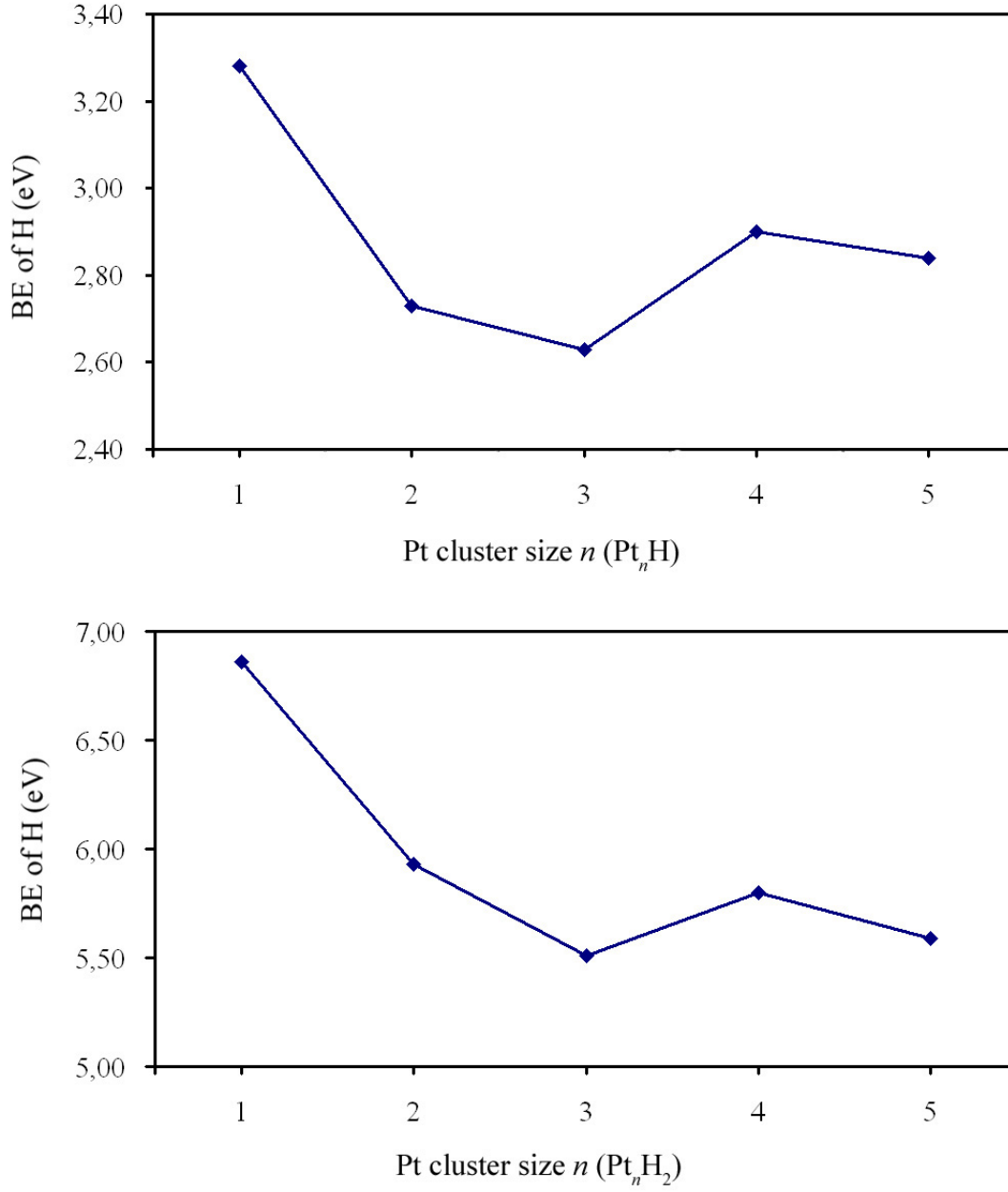


FIG. 3: Binding energies of H (top) and 2H (bottom) atoms on Pt_n clusters.